Electronic Supplementary Information

Efficient formation of [3]pseudorotaxane based on cooperative complexation of dibenzo-24-crown-8 with diphenylviologen axle

Yoko Sakata,* Takaya Ogura and Shigehisa Akine*

* To whom correspondence should be addressed.
E-mail: sakata@se.kanazawa-u.ac.jp
akine@se.kanazawa-u.ac.jp

Experimental

Materials and methods

Reagents and solvents were purchased from commercial sources and used without further purification. ^{1}H NMR spectra were recorded on a Bruker Avance Neo 400 (400 MHz) or a Bruker Avance Neo 600 (600 MHz). ^{13}C NMR spectra were recorded on a Bruker Avance Neo 600 (150 MHz). Chemical shifts were referenced with respect to tetramethylsilane (0 ppm) as an internal standard or the solvent residual peak (^{1}H, 3.31 ppm for CD_2HOD and 1.94 ppm for CD_2HCN; ^{13}C, 1.32 ppm for CD_3CN). ESI-TOF mass spectra were recorded on a Bruker Daltonics micrOTOF II.

The synthetic precursors (1,1′-bis(4-carboxyphenyl)-(4,4′-bipyridinium) dichloride[1] and 1,1′-bis(4-carboxybenzyl)-4,4′-bipyridinium dibromide[2]) and sodium tetrakis[3,5-bis(trifluoromethyl)phenyl]borate[3] were prepared according to the literatures.

X-ray Crystallography

Intensity data were collected on a Bruker SMART APEX II (with Cu Kα radiation, λ = 1.54178 Å). The data were corrected for Lorentz and polarization factors and for absorption by semiempirical methods based on symmetry-equivalent and repeated reflections. The structure was solved by direct methods (SHELXT[4]) and refined by full-matrix least squares on F^2 using SHELXL 2014.[5] Crystallographic data for **A1**•$(DB24C8)_2$•$3CHCl_3$•MeOH•H_2O has been deposited with the Cambridge Crystallographic Data Centre under reference number CCDC 1998063. These data can be obtained free of charge via www.ccdc.cam.ac.uk/data_request/cif (or from the Cambridge Crystallographic Data Centre, 12 Union Road, Cambridge CB2 1EZ, UK).

Synthesis of A1

A solution of sodium tetrakis[3,5-bis(trifluoromethyl)phenyl]borate (1.31 g, 1.48 mmol) in methanol (10 mL) was added to a solution of 1,1′-bis(4-carboxyphenyl)-(4,4′-bipyridinium) dichloride (202 mg, 0.43 mmol) in methanol (50 mL). Water (65 mL) was further added to the mixture and the resulting pale green precipitates were collected by filtration (552 mg, 0.26 mmol, 60%).

^{1}H NMR (600 MHz, CD_3CN) δ 9.23 (d, J = 6.6 Hz, 4H), 8.67 (d, J = 6.6 Hz, 4H), 8.38 (d, J = 8.4 Hz, 4H), 7.90 (d, J = 8.4 Hz, 4H), 7.70–7.67 (m, 24H); ^{13}C {^{1}H} NMR (150 MHz, CD_3CN) δ 166.18, 162.60 (q, $^{1}J_{B–C}$ = 49.8 Hz), 151.65, 146.81, 146.14, 135.65, 134.76, 132.79, 129.93 (q, $^{2}J_{F–C}$ = 32.2 Hz), 128.48, 126.08, 125.46 (q, $^{1}J_{F–C}$ = 270.1 Hz), 118.69; Anal. Calcd for $C_{88}H_{42}B_2F_{48}N_2O_4$•$5H_2O$: C, 47.72; H, 2.37; N, 1.26. Found: C, 47.73; H, 2.25; N, 1.53.

Synthesis of A2

A solution of sodium tetrakis[3,5-bis(trifluoromethyl)phenyl]borate (1.00 g, 1.13 mmol) in methanol (20 mL) was added to a solution of 1,1′-bis(4-carboxybenzyl)-4,4′-bipyridinium dibromide (205 mg, 0.35

mmol) in 50% aqueous methanol (40 mL). After the solution was concentrated to reduce the amount of methanol, water (70 mL) was added to the mixture. The resulting pale yellow precipitates were isolated by centrifugation and the remaining solvent was removed in vacuo (665 mg, 0.31 mmol, 89%).

^{1}H NMR (600 MHz, CD_3CN) δ 8.95 (d, J = 6.9 Hz, 4H), 8.36 (d, J = 6.9 Hz, 4H), 8.10 (d, J = 8.4 Hz, 4H), 7.70–7.67 (m, 24H), 7.57 (d, J = 8.4 Hz, 4H), 5.88 (s, 4H); ^{13}C {^{1}H} NMR (150 MHz, CD_3CN) δ 166.95, 162.60 (q, $^{1}J_{B–C}$ = 49.5 Hz), 151.44, 146.84, 138.21, 135.65, 132.64, 131.61, 130.37, 129.93 (q, $^{2}J_{F–C}$ = 31.4 Hz), 128.62, 125.46 (q, $^{1}J_{F–C}$ = 270.1 Hz), 118.69, 65.12; Anal. Calcd for $C_{90}H_{46}B_2F_{48}N_2O_4$•$2H_2O$: C, 49.38; H, 2.30; N, 1.28. Found: C, 49.64; H, 2.57; N, 1.30.

ESI-TOF mass spectra of [2]pseudorotaxane A1•(24C8) and [3]pseudorotaxane A1•(24C8)$_2$

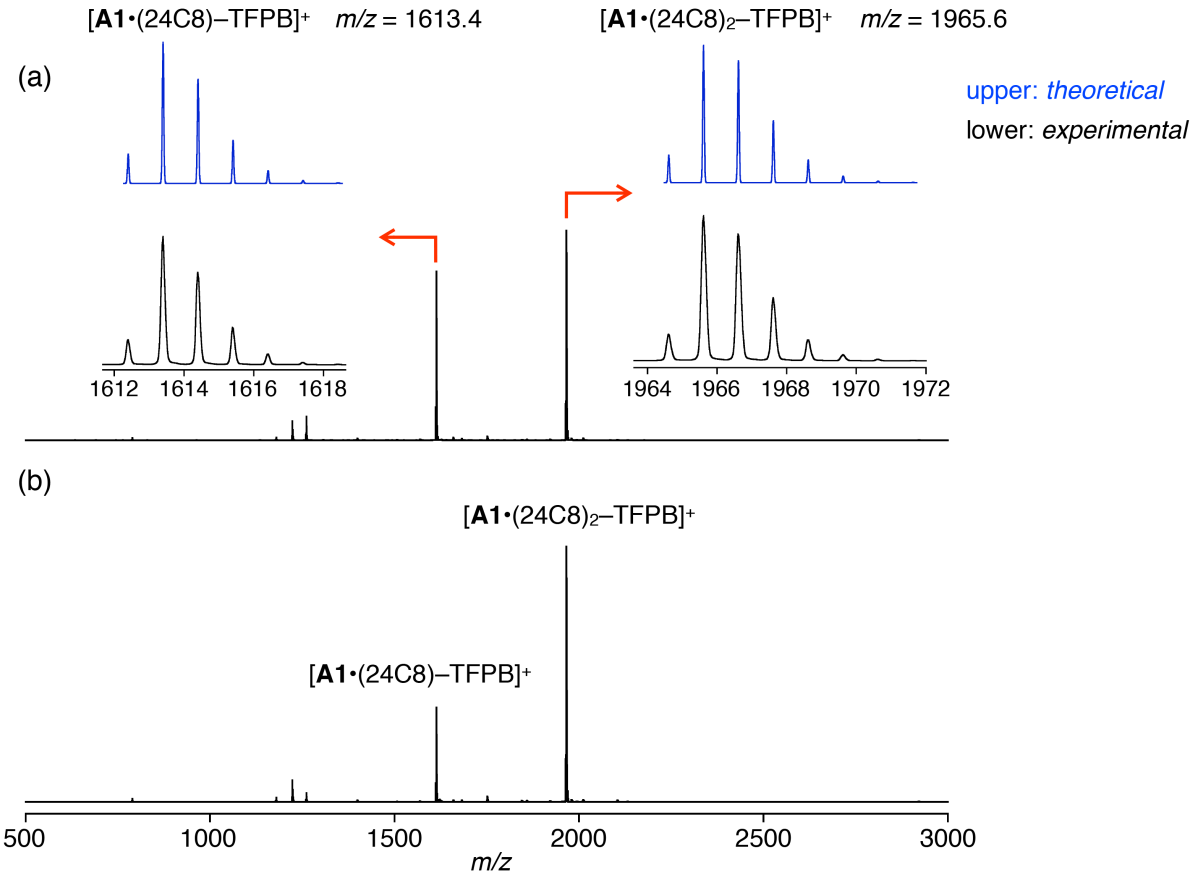

Fig. S1 ESI-TOF mass spectra of **A1** in the presence of 24C8 (a, 3 equiv; b, 5 equiv).

Crystallographic analysis of A1•(DB24C8)$_2$

Table S1 Crystallographic data for **A1**•(DB24C8)$_2$•3CHCl$_3$•MeOH•H$_2$O.

	A1•(DB24C8)$_2$•3CHCl$_3$•MeOH•H$_2$O
Formula	$C_{141}H_{119}B_2Cl_9F_{48}N_2O_{23}$
Formula weight	3462.05
Temperature (K)	90
Crystal size (mm^3)	0.50 × 0.25 × 0.10
Crystal system	triclinic
Space group	$P\bar{1}$
a (Å)	20.1230(11)
b (Å)	20.4221(10)
c (Å)	21.1299(11)
α (deg)	81.209(2)
β (deg)	76.368(2)
γ (deg)	72.895(2)
V (Å^3)	8032.9(7)
Z	2
D_{calcd} (g cm^{-3})	1.431
Collected reflections	159701
Unique reflections	28315
R_{int}	0.0547
$2\theta_{max}$	134.138
F_{000}	3516
μ(CuKα) (mm^{-1})	2.496
Limiting indices	$-20 \le h \le 23$
	$-24 \le k \le 24$
	$-25 \le l \le 25$
Restraints/parameters	585/2444
Goodness of fit (F^2)	1.045
$R1$ ($I > 2\sigma(I)$)	0.0757
$wR2$ ($I > 2\sigma(I)$)	0.2182
$R1$ (all data)	0.0810
$wR2$ (all data)	0.2238

Table S2 Selected C–H•••π distances in the crystal structure of **A1**•$(DB24C8)_2$ (Å).

C–H•••Ph**X**	*d*(H•••Ph**X**)[1]
C9–H7•••Ph**A** (C61–C66)	2.663
C11–H8•••Ph**B** (C49–C54)	2.930
C14–H10•••Ph**C** (C25–C30)	2.739
C17–H13•••Ph**D** (C37–C42)	2.832

[1]The distance between the mean plane of phenylene ring **X** and hydrogen atom.

Table S3 Selected hydrogen bond distances in the crystal structure of **A1**•$(DB24C8)_2$ (Å).

C–H•••O	*d*(H•••O)
Phenyl C–H•••O	
C4–H3•••O5	2.924
C4–H3•••O12	2.594
C6–H4•••O8	2.514
C6–H4•••O9	2.708
C19–H14•••O13	2.631
C19–H14•••O20	2.701
C23–H17•••O16	2.679
C23–H17•••O17	2.539
Pyridinium C–H•••O	
C8–H6•••O10	2.581
C8–H6•••O11	2.112
C12–H9•••O6	2.485
C12–H9•••O7	2.135
C15–H11•••O14	2.437
C15–H11•••O15	2.138
C16–H12•••O18	2.468
C16–H12•••O19	2.180

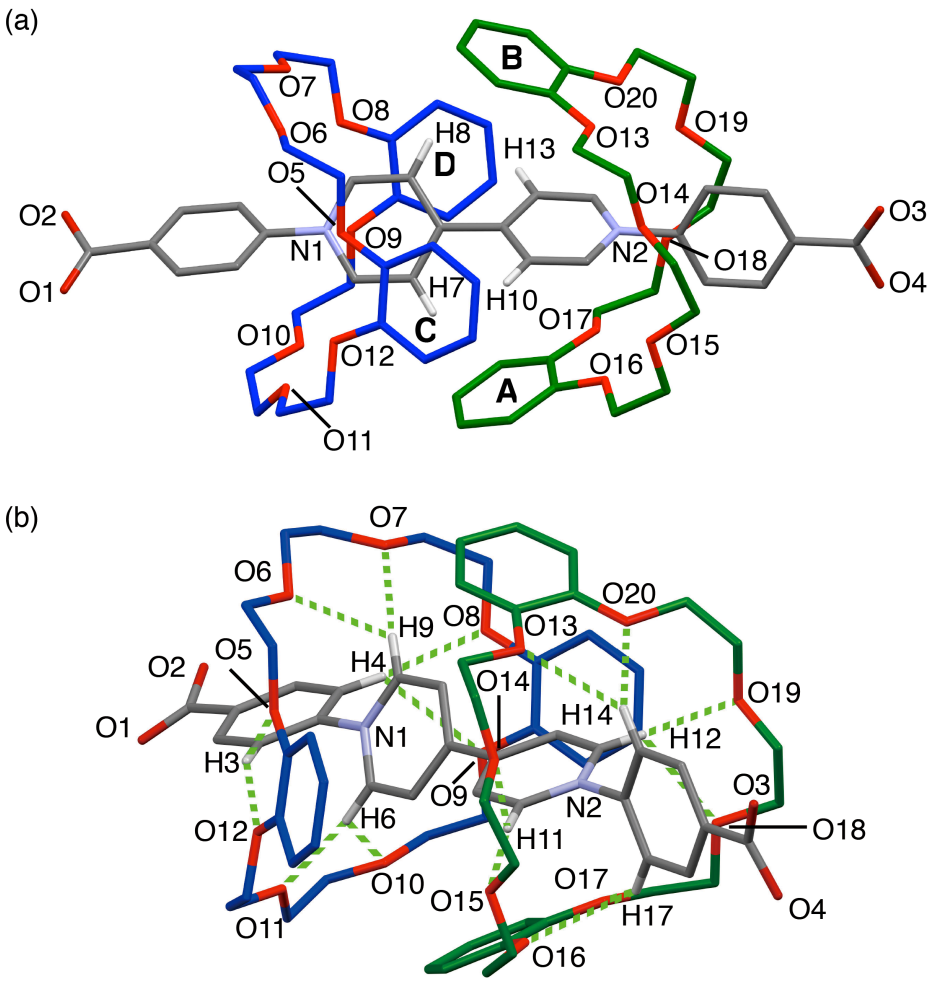

Fig. S2 Crystal structure of **A1**•$(DB24C8)_2$ (capped stick models). Hydrogen atoms, solvent molecules and TFPB anions are omitted for clarity. Hydrogen atoms participating in the C–H•••π and C–H•••O interactions are shown in (a) and (b), respectively. The green dotted lines indicate the C–H•••O hydrogen bonds (for the C–H•••π and C–H•••O distances, see Table S2 and S3, respectively).

^{1}H NMR spectral changes of A1 upon the addition of 24C8 in $CDCl_3/CD_3CN$ (4:1)

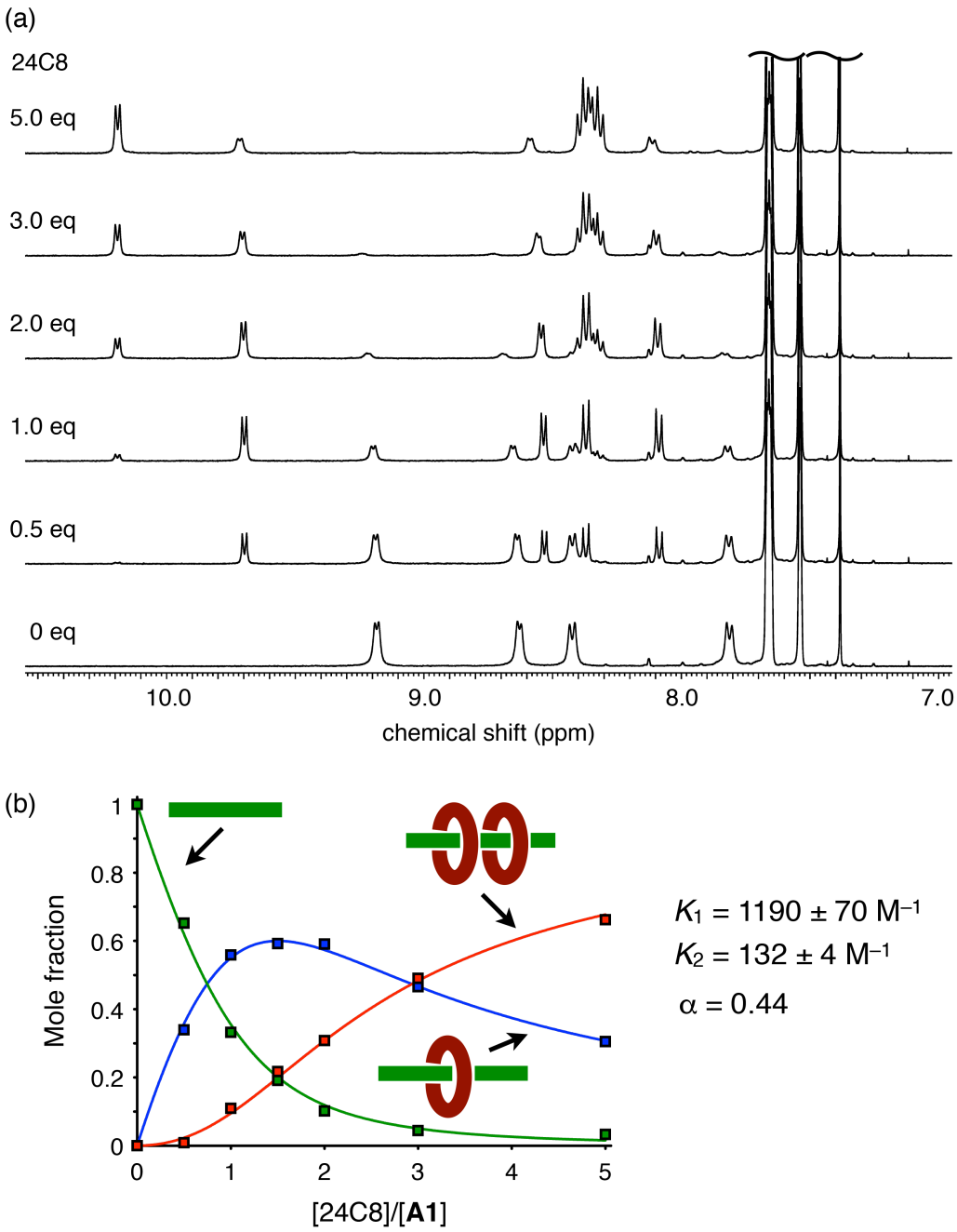

Fig. S3 (a) ^{1}H NMR spectral changes of **A1** upon the addition of 24C8 (400 MHz, 25 °C, $CDCl_3/CD_3CN$ (4:1), [**A1**] = 5 mM), (b) Nonlinear curve fitting of the changes of the mole fractions obtained from the titration study.

^{1}H NMR spectral changes of A1 upon the addition of DB24C8 in $CDCl_3/CD_3CN$ (4:1)

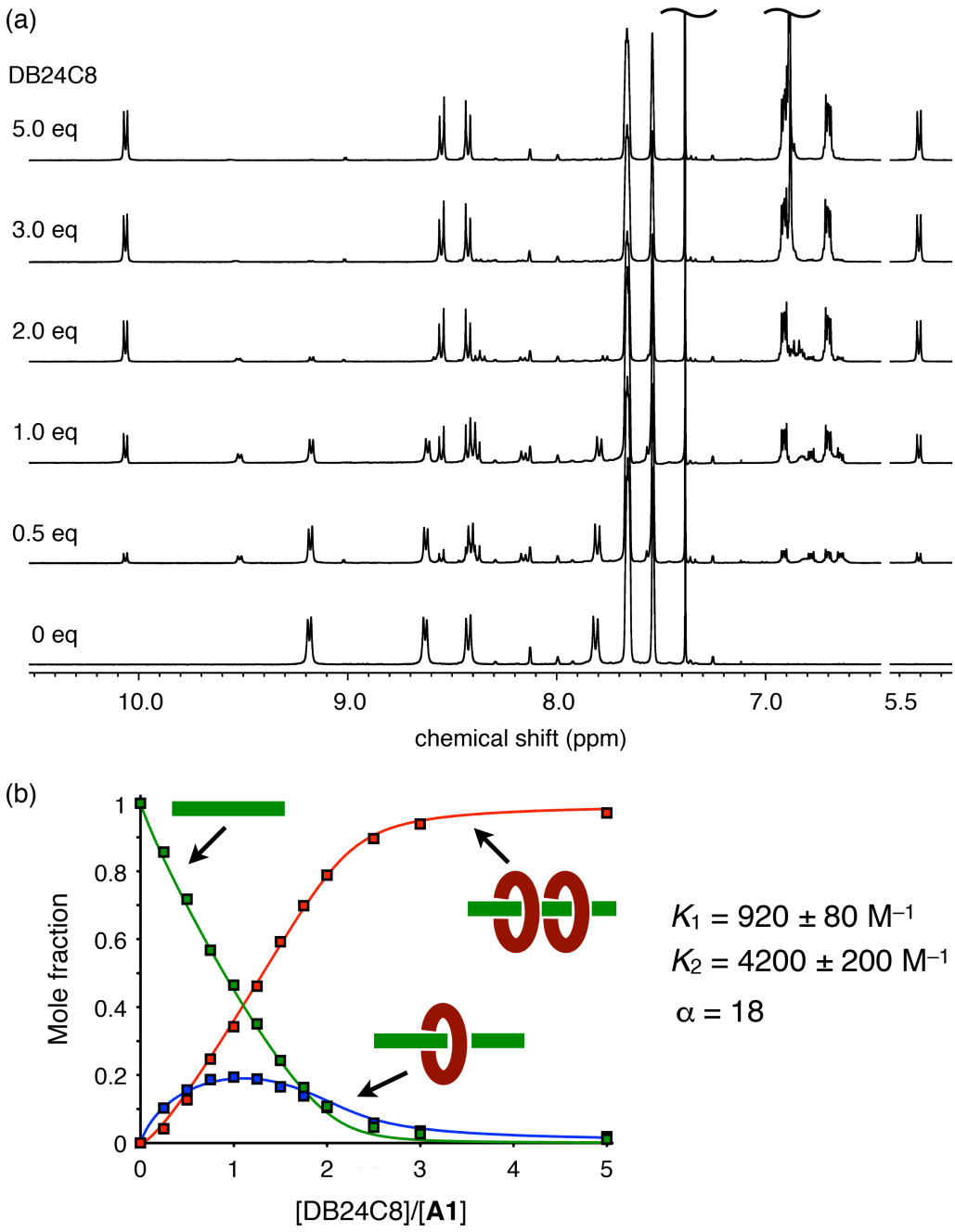

Fig. S4 (a) ^{1}H NMR spectral changes of **A1** upon the addition of DB24C8 (400 MHz, 25 °C, $CDCl_3/CD_3CN$ (4:1), [**A1**] = 5 mM), (b) Nonlinear curve fitting of the changes of the mole fractions obtained from the titration study.

^{1}H NMR spectral changes of A1 upon the addition of DN24C8 in $CDCl_3/CD_3CN$ (4:1)

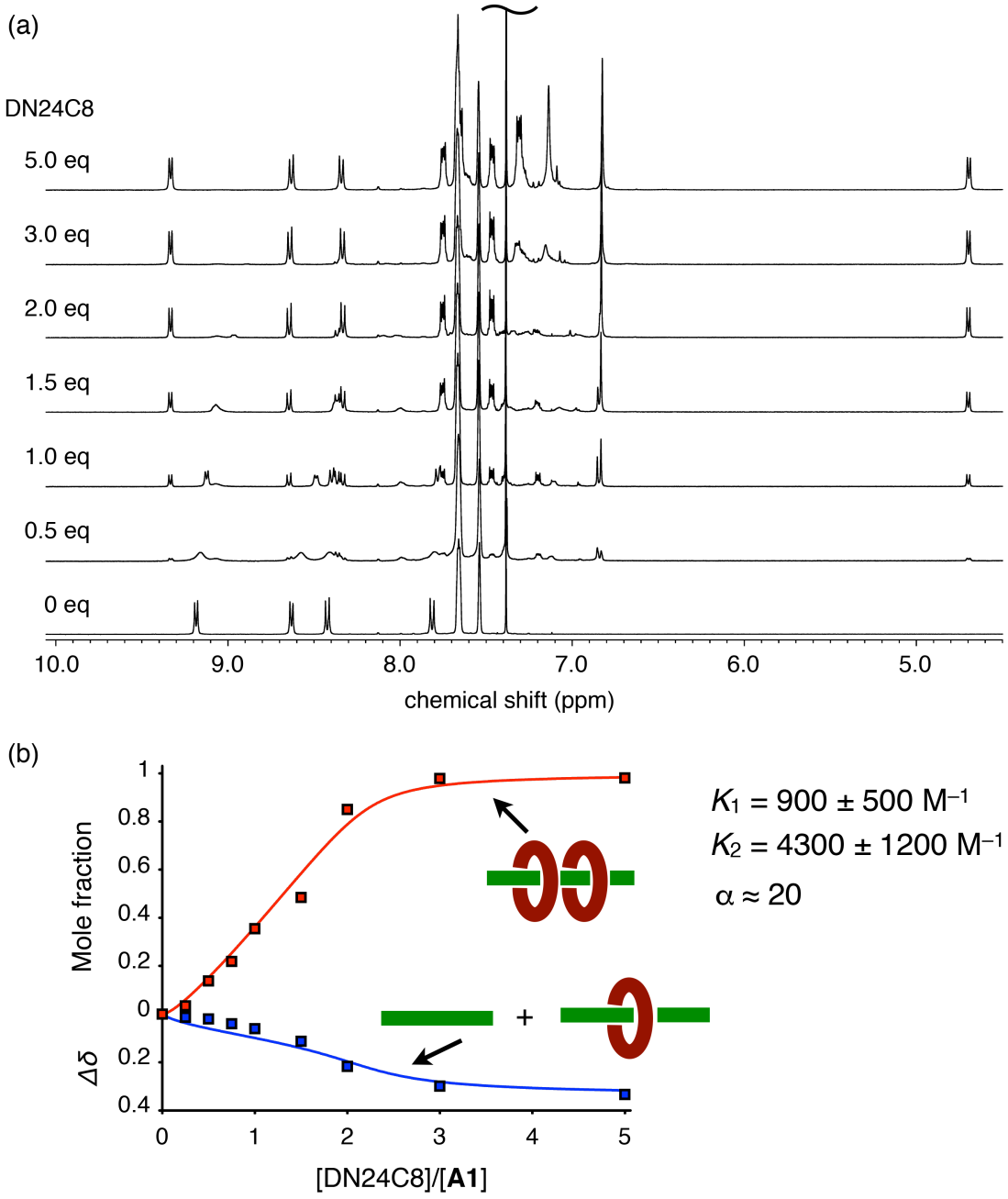

Fig. S5 (a) ^{1}H NMR spectral changes of **A1** upon the addition of DN24C8 (400 MHz, 25 °C, $CDCl_3/CD_3CN$ (4:1), [**A1**] = 5 mM), (b) Nonlinear curve fitting of the changes of the mole fractions and chemical shift obtained from the titration study.[#]

While the equilibrium between free axle **A1** and [2]pseudorotaxane (DN24C8)•**A1** is fast on the NMR time scale, the signals for [3]pseudorotaxane $(DN24C8)_2$•**A1** were independently observed. Thus, the binding constants were determined based on both the chemical shift change of **A1** and the change of the mole fraction of the [3]pseudorotaxane.

^{1}H NMR spectral changes of A1 upon the addition of DB30C10 in $CDCl_3/CD_3CN$ (4:1)

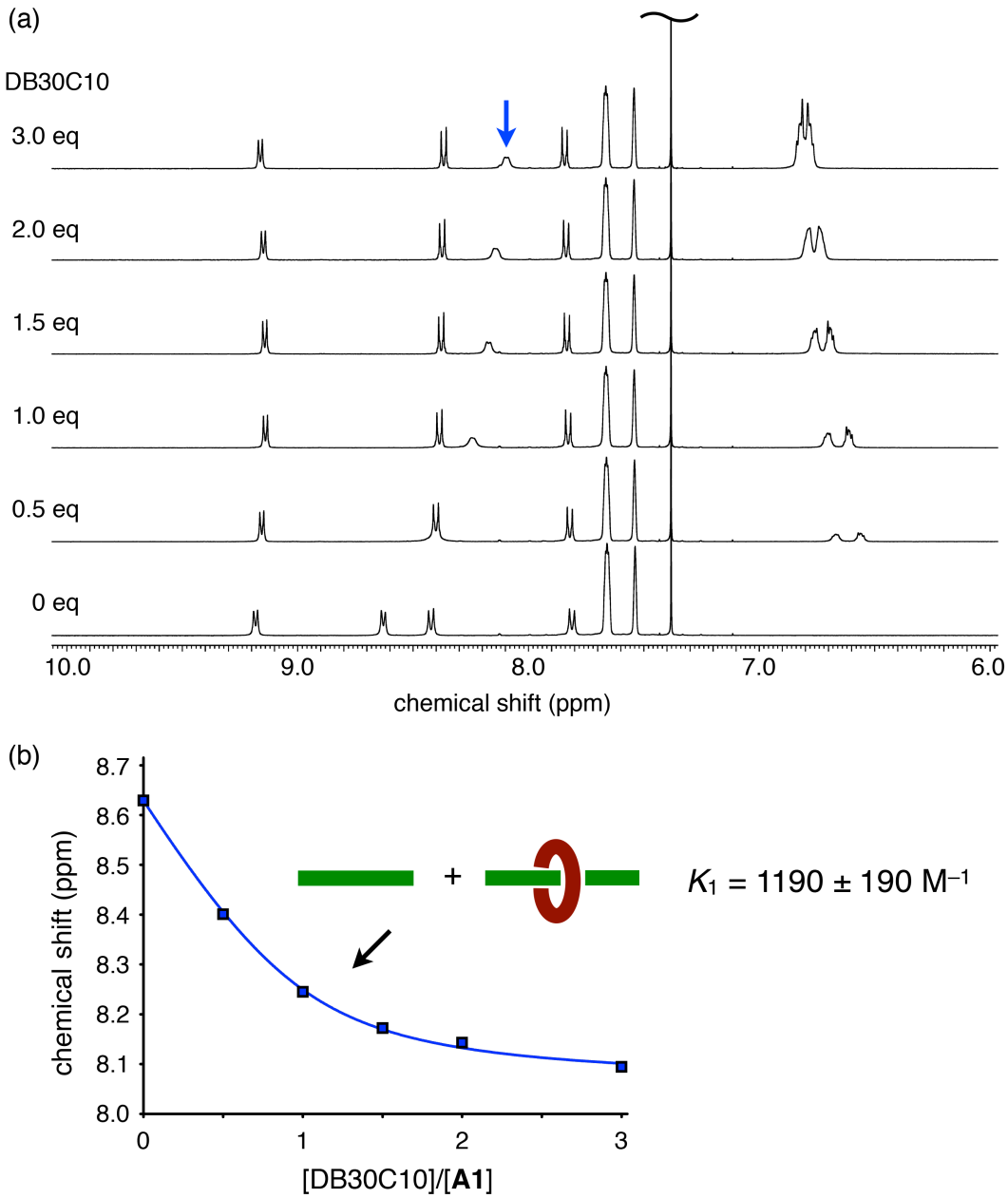

Fig. S6 (a) ^{1}H NMR spectral changes of **A1** upon the addition of DB30C10 (400 MHz, 25 °C, $CDCl_3/CD_3CN$ (4:1), [**A1**] = 5 mM), (b) Nonlinear curve fitting of the chemical shift changes obtained from the titration study.

^{1}H NMR spectral changes of A2 upon the addition of DB24C8 in $CDCl_3/CD_3CN$ (4:1)

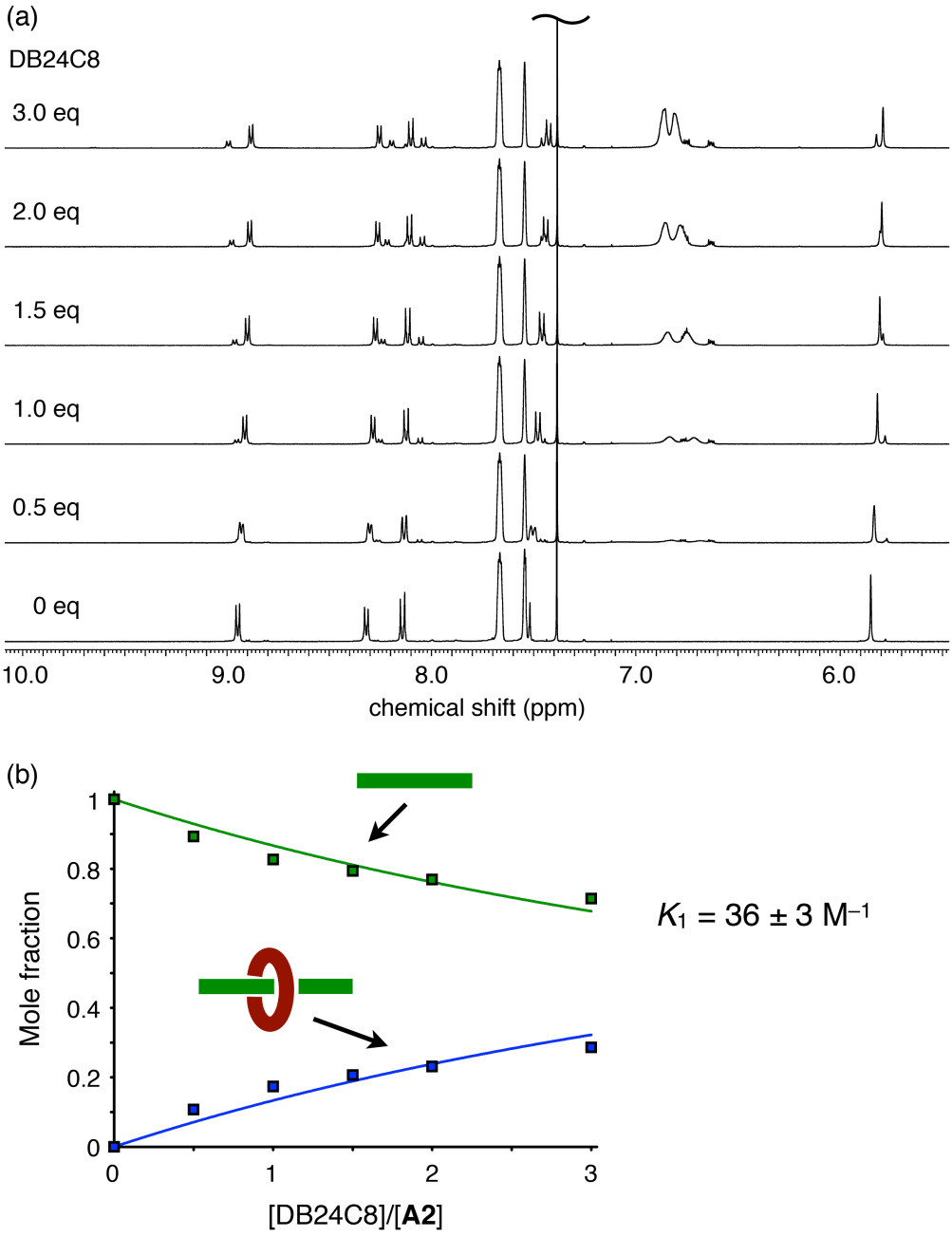

Fig. S7 (a) ^{1}H NMR spectral changes of **A2** upon the addition of DB24C8 (400 MHz, 25 °C, $CDCl_3/CD_3CN$ (4:1), [**A2**] = 5 mM), (b) Nonlinear curve fitting of the changes of the mole fractions obtained from the titration study.

^{1}H NMR spectral changes of A2 upon the addition of DN24C8 in $CDCl_3/CD_3CN$ (4:1)

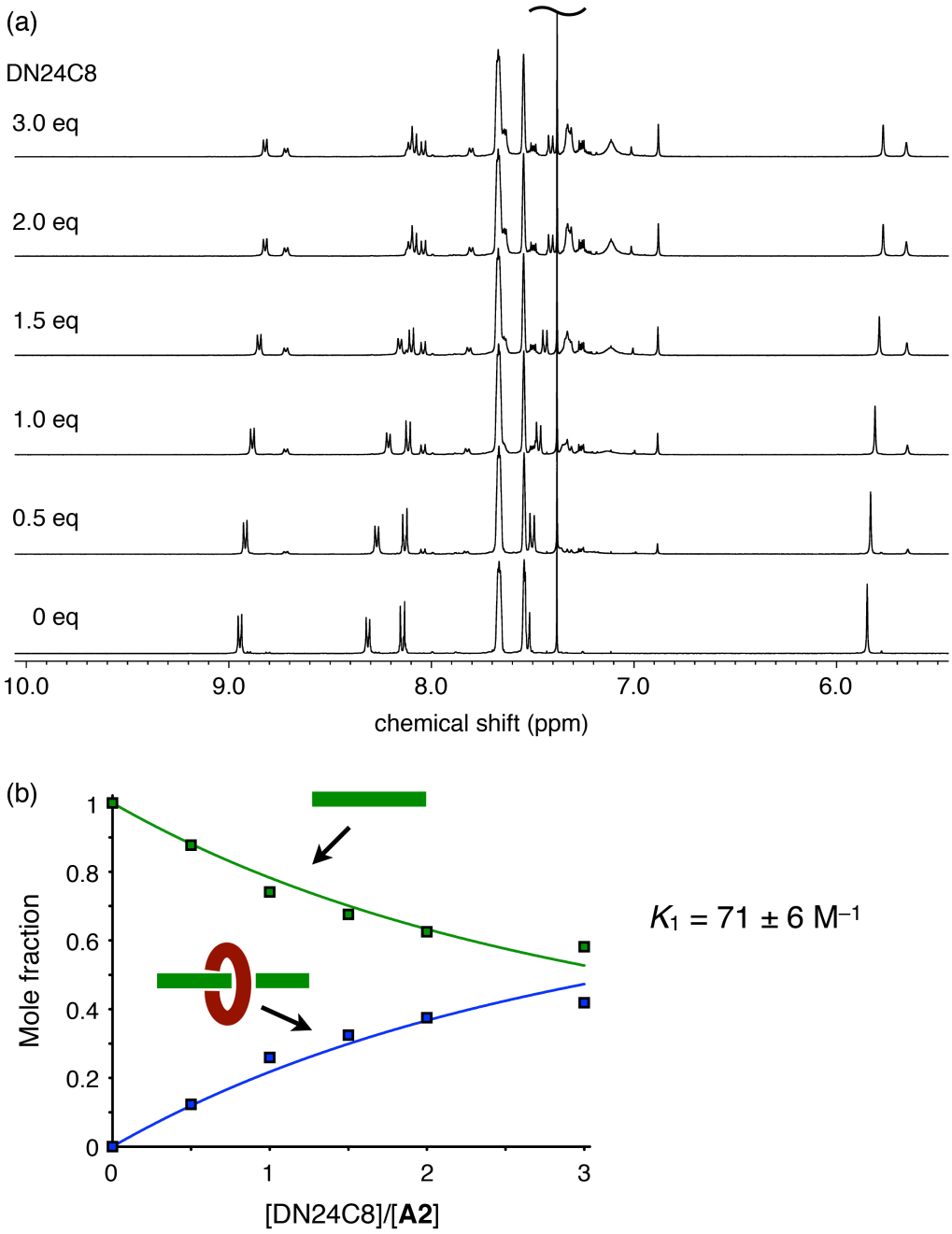

Fig. S8 (a) ^{1}H NMR spectral changes of **A2** upon the addition of DN24C8 (400 MHz, 25 °C, $CDCl_3/CD_3CN$ (4:1), [**A2**] = 5 mM), (b) Nonlinear curve fitting of the changes of the mole fractions obtained from the titration study.

^{1}H NMR spectral changes of A1 upon the addition of DB24C8 in CD_3CN

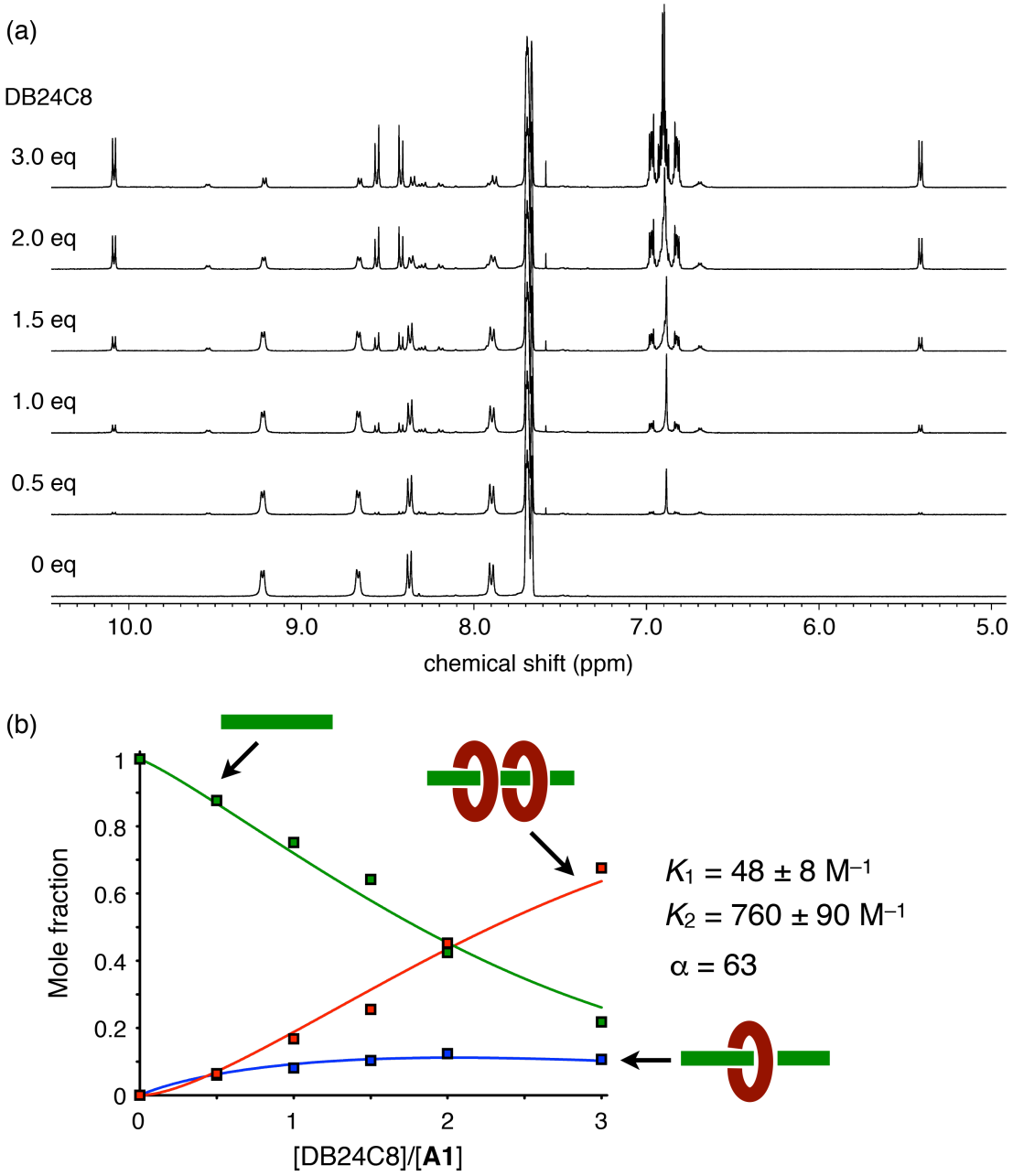

Fig. S9 (a) ^{1}H NMR spectral changes of **A1** upon the addition of DB24C8 (400 MHz, 25 °C, CD_3CN, [**A1**] = 5 mM), (b) Nonlinear curve fitting of the changes of the mole fractions obtained from the titration study.

^{1}H NMR spectral changes of A1 upon the addition of DB24C8 in $CDCl_3/CD_3OD$ (4:1)

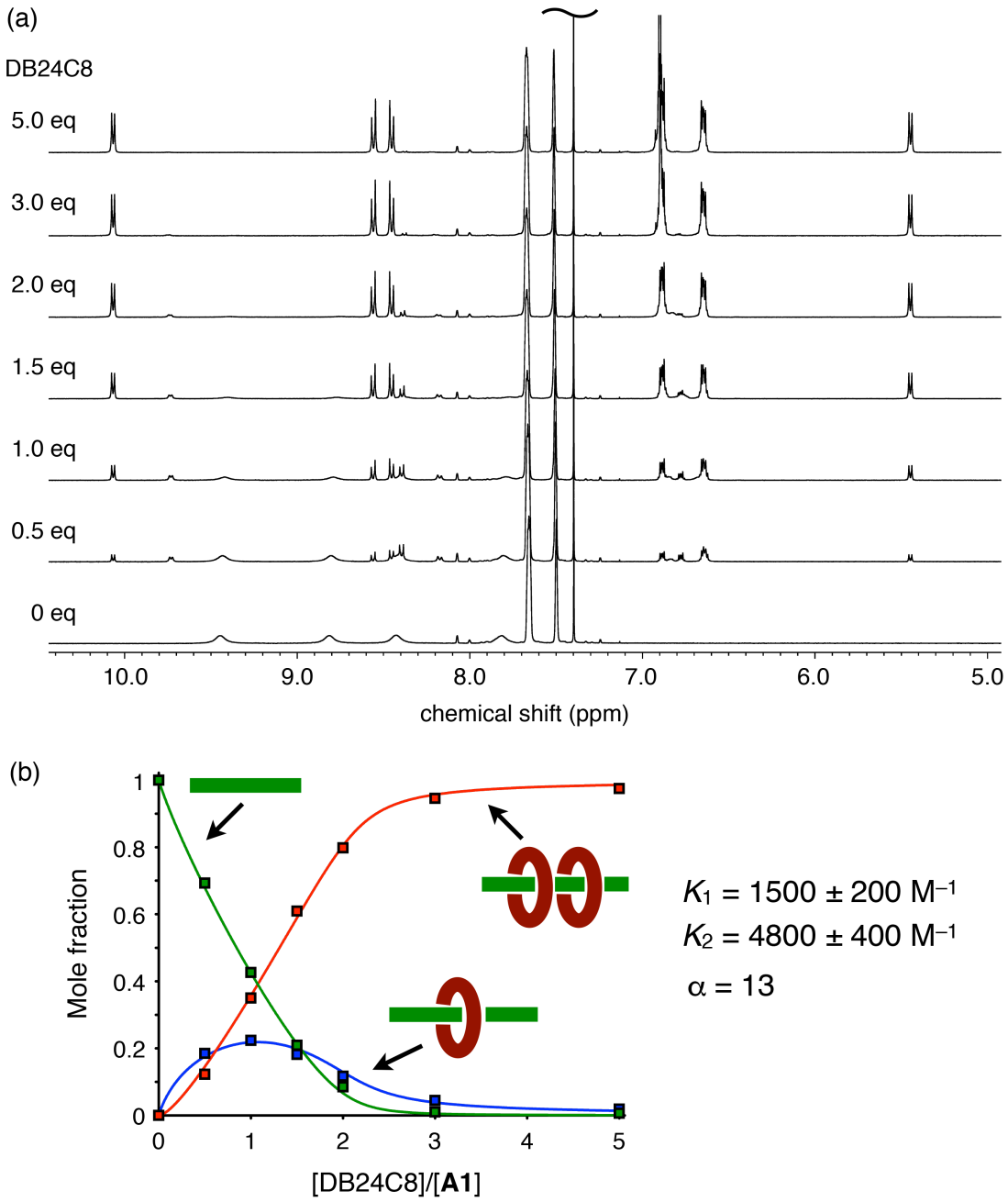

Fig. S10 (a) ^{1}H NMR spectral changes of **A1** upon the addition of DB24C8 (400 MHz, 25 °C, $CDCl_3/CD_3OD$ (4:1), [**A1**] = 5 mM), (b) Nonlinear curve fitting of the changes of the mole fractions obtained from the titration study.

^{1}H NMR spectral changes of A1 upon the addition of DB24C8 in CD_3OD

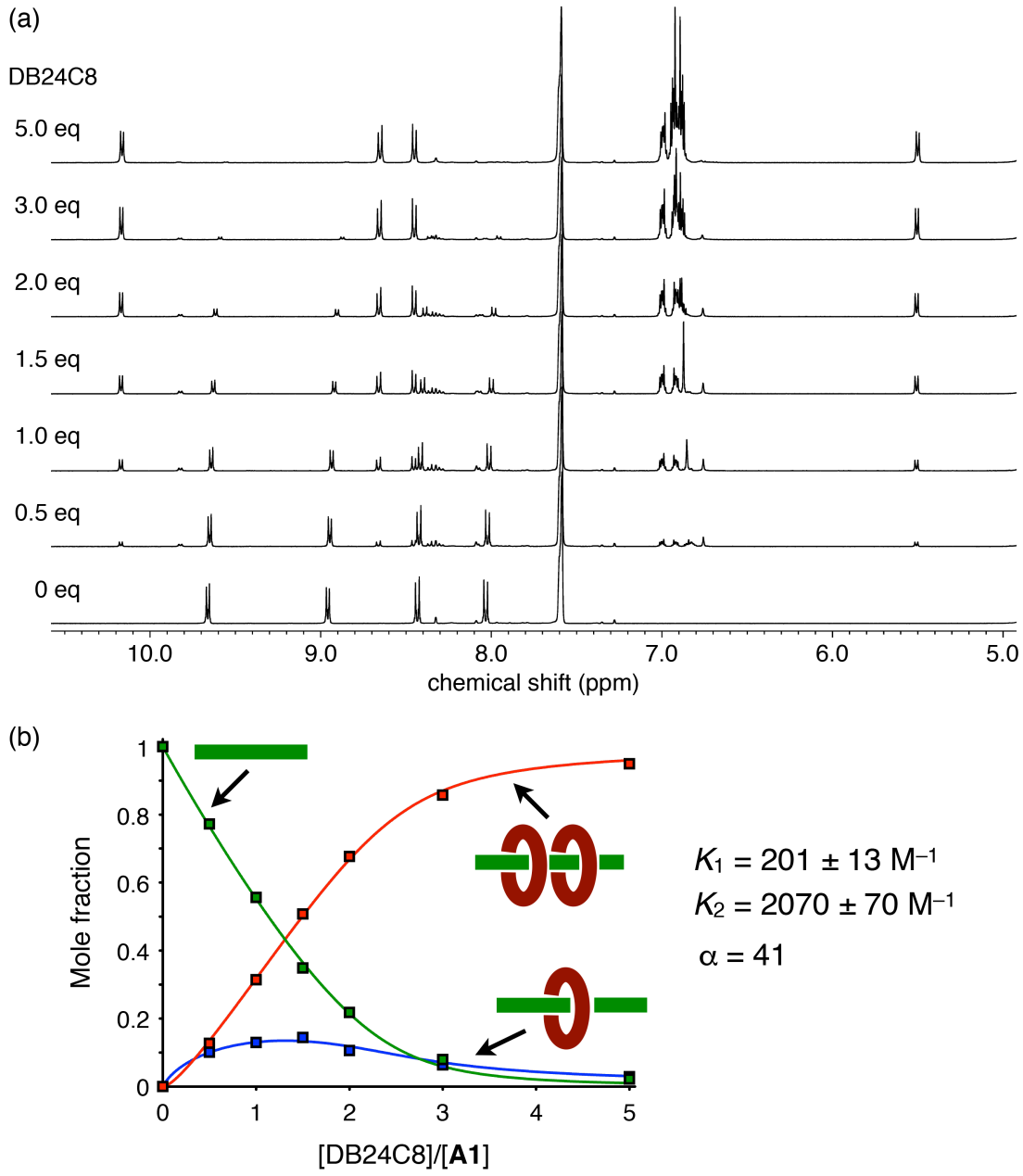

Fig. S11 (a) ^{1}H NMR spectral changes of **A1** upon the addition of DB24C8 (400 MHz, 25 °C, CD_3OD, [**A1**] = 5 mM), (b) Nonlinear curve fitting of the changes of the mole fractions obtained from the titration study.

^{1}H NMR spectral changes of A1 upon the addition of DB24C8 in $CDCl_3$/DMSO-d_6 (4:1)

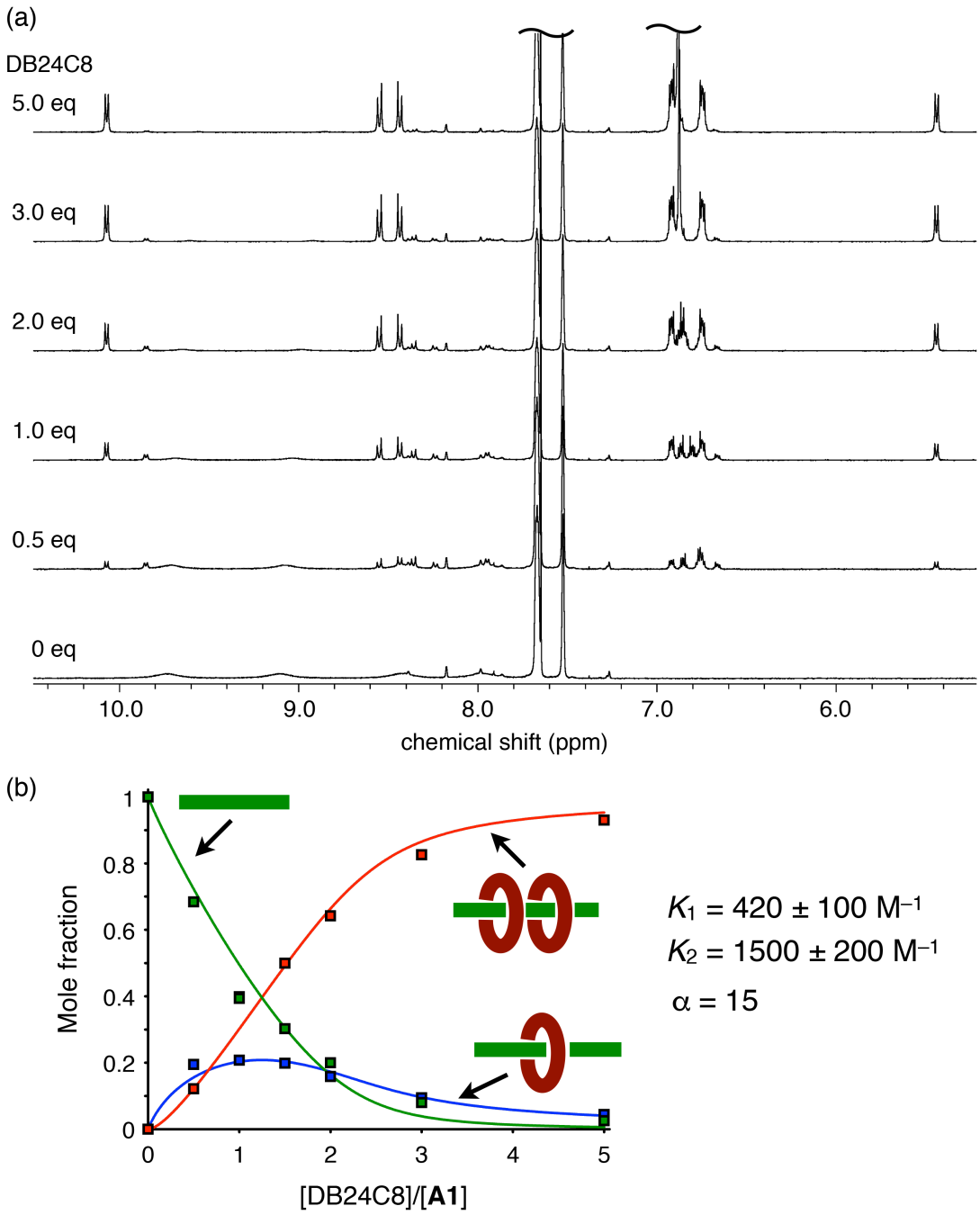

Fig. S12 (a) ^{1}H NMR spectral changes of **A1** upon the addition of DB24C8 (400 MHz, 25 °C, $CDCl_3$/DMSO-d_6 (4:1), [**A1**] = 5 mM), (b) Nonlinear curve fitting of the changes of the mole fractions obtained from the titration study.

^{1}H NMR spectral changes of A1 upon the addition of DB24C8 in DMSO-d_6

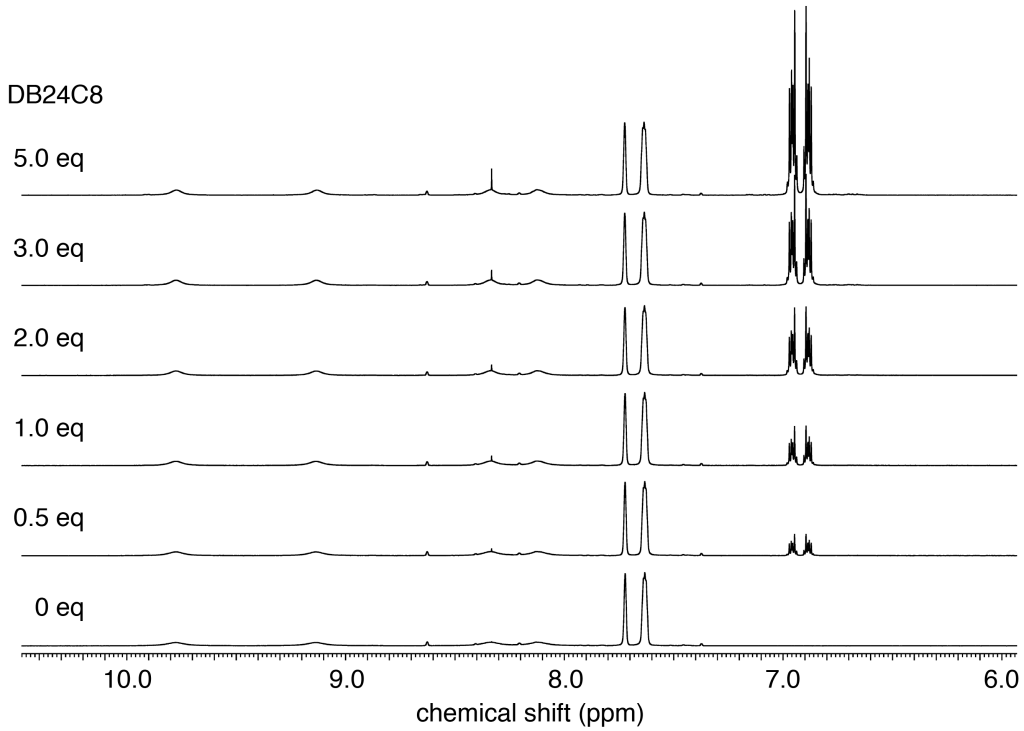

Fig. S13 ^{1}H NMR spectral changes of **A1** upon the addition of DB24C8 (400 MHz, 25 °C, DMSO-d_6, [**A1**] = 5 mM).

^{1}H NOESY spectrum of a 1:5 mixture of A1 and DB24C8

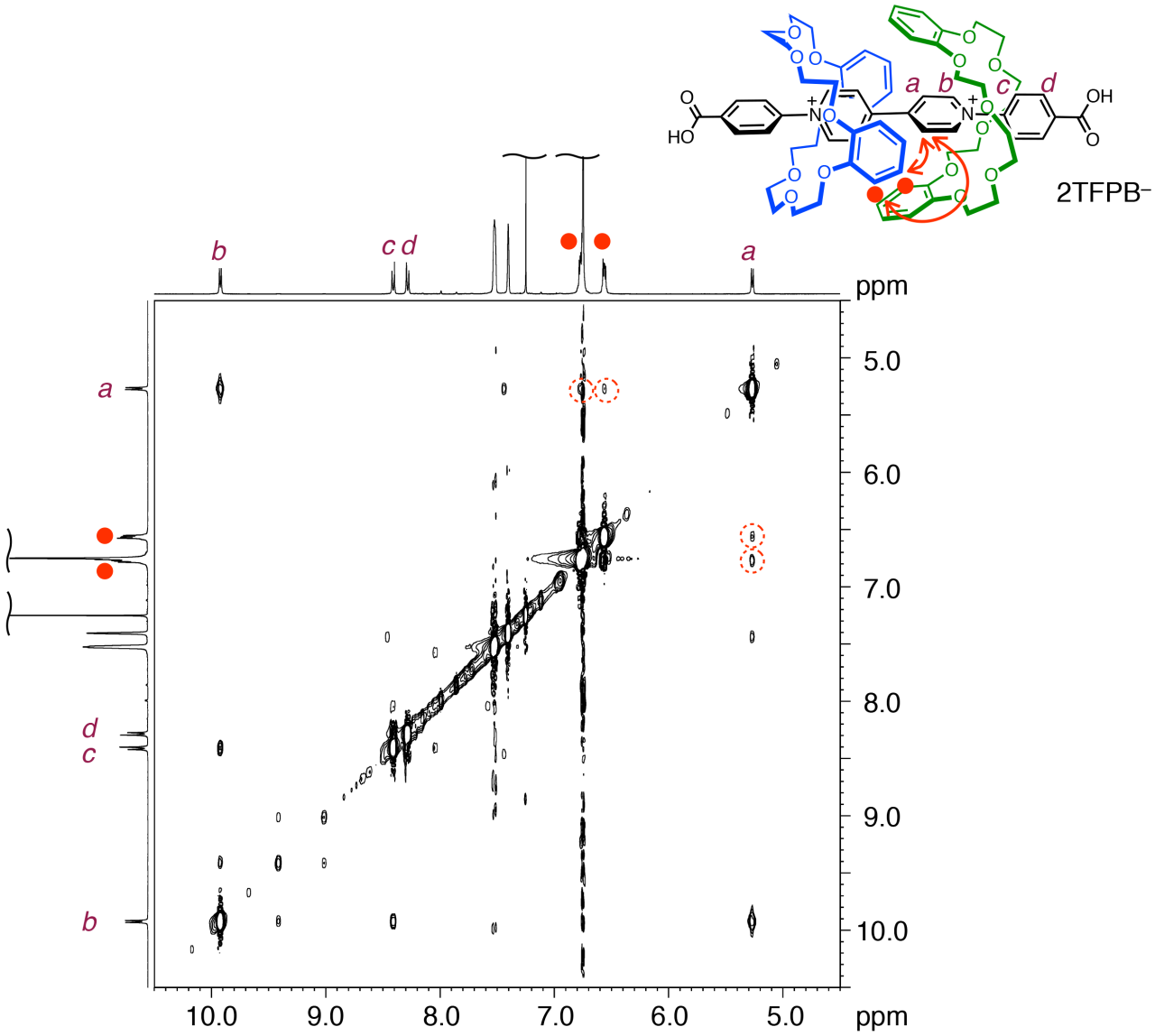

Fig. S14 ^{1}H NOESY spectrum of a 1:5 mixture of **A1** and DB24C8 (400 MHz, 25 °C, $CDCl_3/CD_3CN$ (4:1), [**A1**] = 5 mM).

ESI-TOF mass spectrum of [3]rotaxane R1•(DB24C8)$_2$

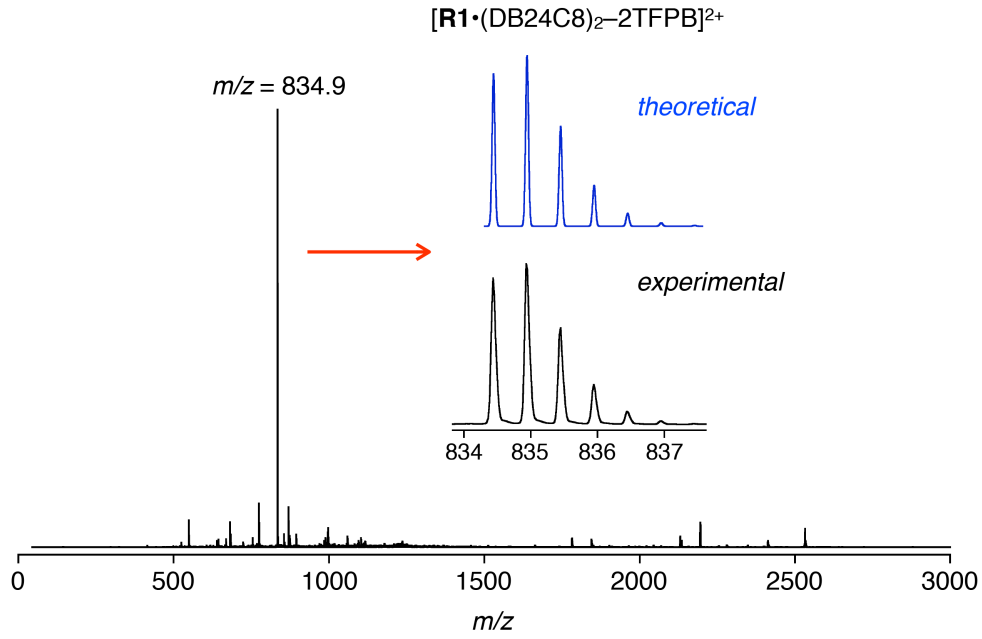

Fig. S15 ESI-TOF mass spectrum of **R1**•(DB24C8)$_2$.

References

[1] J.-J. Liu, Y.-F. Guan, M.-J. Lin, C.-C. Huang and W.-X. Dai, *Cryst. Growth Des.,* 2015, **15**, 5040–5046.

[2] M. R. Geraskina, A. S. Dutton, M. J. Juetten, S. A. Wood and A. H. Winter, *Angew. Chem., Int. Ed.*, 2017, **56**, 9435–9439.

[3] H. Nishida, N. Takada, M. Yoshimura, T. Sonoda and H. Kobayashi, *Bull. Chem. Soc. Jpn.,* 1984, **57**, 2600–2604.

[4] G. M. Sheldrick, SHELXT – Integrated space-group and crystal-structure determination. *Acta Crystallogr.* 2015, **A71**, 3–8.

[5] G. M. Sheldrick, Crystal structure refinement with *SHELXL. Acta Crystallogr.* 2015, **C71**, 3–8.